

QUANTITATIVE MUELLER MATRIX POLARIMETRY TECHNIQUES FOR BIOLOGICAL TISSUES

HONGHUI HE^{*,†}, NAN ZENG^{*,†}, DONGZHI LI^{*,†,‡}, RAN LIAO^{*,†}
and HUI MA^{*,†,‡,§}

**Shenzhen Key Laboratory for Minimal Invasive Medical Technologies
Shenzhen 518055, P. R. China*

*†Laboratory of Optical Imaging and Sensing, Graduate School at Shenzhen
Tsinghua University, Shenzhen 518055, P. R. China*

*‡Department of Physics, Tsinghua University
Beijing 100084, P. R. China*

§mahui@tsinghua.edu.cn

Accepted 12 June 2012
Published 10 August 2012

We propose and conduct both the rotating linear polarization imaging (RLPI) and Mueller matrix transformation (MMT) measurements of different biological tissue samples, and testify the capability of the Mueller matrix polarimetry for the anisotropic scattering media. The independent parameters extracted from the RLPI and MMT techniques are compared and analyzed. The tissue experimental results show that the parameters are closely related to the structural characteristics of the turbid scattering media, including the sizes of the scatterers, the angular distribution and order of alignment of the fibers. The results and conclusions in this paper may provide a potential method for the detection of precancerous and early stage cancerous tissues. Also, such studies represent the Mueller matrix transformation procedure which results in a set of parameters linking up the Mueller matrix elements to the structural and optical properties of the media.

Keywords: Polarization; scattering; Mueller matrix; biological tissues.

1. Introduction

Recently, the potential applications of the non-invasive optical imaging techniques using polarized light have caused special concern in biomedical research.¹⁻³ Since the polarization state of light can be affected by the structures of biological tissues, these polarized imaging techniques provide

additional structural information of tissues. Most biological tissues contain anisotropic components, such as the myofibrils in skeletal muscles, the collagen fibers in tendons, and axon. Therefore, for the studies of biomedical optics and its applications for therapeutics and diagnostics purposes, one needs to use proper imaging techniques to extract the

§Corresponding author.

structural information of the samples. In the past two decades, the Mueller matrix has been used as a powerful tool to extract the quantitative information of isotropic turbid scattering media, such as the scattering coefficient and the size distributions of the scatterers.^{4–6} In previous studies, we have demonstrated that the Mueller matrix can also be used to characterize the anisotropic properties of a sphere-cylinder scattering medium.^{7–9} Using the experimental and Monte Carlo simulated results, we examine in detail the characteristic features in each Mueller matrix element and the influence of different parameters on the Mueller matrix. The Mueller matrix can be used to characterize quantitatively the structural and optical properties of anisotropic biological tissues.

Despite of the potential utility, a main obstacle for the application of the Stokes–Mueller polarimetry is that, the physical meaning of the Mueller matrix elements is often unclear, especially for the anisotropic scattering materials. Many structural parameters may affect the same Mueller matrix element simultaneously, and the combined effects can hardly be separated. To deal with this problem, a quantitative method called Mueller matrix decomposition has been proposed and used for some biomedical purposes.^{10–12} Meanwhile, we proposed an imaging technique called rotating linear polarization imaging (RLPI), which provides a group of parameters related to certain structures of the anisotropic media.^{13,14} These parameters can be expressed as analytical functions of the Mueller matrix elements. Both the experiments on biological tissues and Monte Carlo simulations have testified the powerful utility of the RLPI method. Recently, we have found that the Mueller matrix elements of the anisotropic scattering medium can be transformed to other unique trigonometric forms, and three independent parameters can be extracted. These parameters are related to the anisotropy, direction and sizes of the scatterers. Also, some preliminary experimental results have shown that, the Mueller matrix transformation (MMT) technique is a potential diagnosis method for biomedical research.

2. Method and Materials

Among several representations of polarization, which include the Mueller matrix, Jones matrix and Poincare sphere, the Stokes vector–Mueller matrix

method is believed to be effective to quantitatively describe the structure-related polarization features of a scattering turbid medium. In Stokes–Mueller method, the polarization state of incident or scattered light is represented by a four-component Stokes vector, then the polarization-related features of a scattering medium can be described by a 4×4 Mueller matrix.¹⁵ Therefore, by measuring the Mueller matrices, a deep insight into the polarization characteristics for turbid media is provided, and some structural parameters of the samples, such as the scattering coefficient or sizes of the scatterers, can be extracted.

The experimental set-up takes a typical configuration for RLPI, which can also be used for backscattering Mueller matrix measurement. As shown in Fig. 1, a 650 nm 1 W LED is the light source. A linear polarizer (P1) is used to control the polarization states of the incident light. The incident light illuminates the sample at about 25 degree to the normal for the elimination of the surface reflection. The polarization states of the scattered light are controlled by a second linear polarizer (P2). Then the backscattering photons are steered to and recorded by a 12 bit CCD camera to produce the reflectance images of the samples. For both the RLPI and MMT measurements, three incident polarization states are achieved: Horizontal linear (H), vertical linear (V), and 45 degree linear (P), then three polarization states correspondent to the incident lights are measured. In this paper, we conduct both the RLPI and MMT techniques for biological samples at the same time. The RLPI technique has

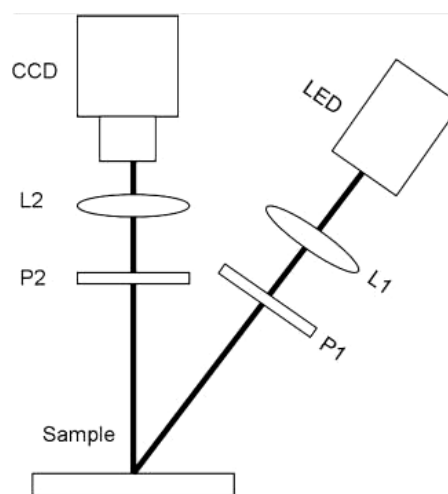


Fig. 1. Schematics of the experimental set-up for both the RLPI and MMT measurements: L-lens, P-polarizer.

been introduced and testified in some previous publications and is summarized briefly here.^{10,11} Based on the definition and the trigonometric forms of the linear polarization difference (LPD), four independent parameters can be acquired:

$$\begin{aligned} A &= [B^2 - (m_{22}m_{33} - m_{23}m_{32})^2]^{1/2}, \\ B &= \frac{(m_{22}^2 + m_{23}^2 + m_{32}^2 + m_{33}^2)}{2}, \\ C &= \sqrt{(m_{21}^2 + m_{31}^2)}, \\ \tan \varphi_3 &= m_{31}/m_{21}. \end{aligned}$$

Experiments for biological samples and Monte Carlo simulations based on sphere-cylinder scattering model (SCSM) have shown that, these RLPI parameters can be used to reflect the optical and structural properties of the scattering media.⁷ Moreover, using the parameter A and B , a normalized indicator for the anisotropic structures can be defined:

$$G = \frac{A}{B}.$$

The RLPI technique results in a set of parameters which can be explicitly expressed as functions of Mueller matrix elements and are sensitive to specific properties of the anisotropic media. The relation between the RLPI method and Mueller matrix elements implies a transformation of the Mueller matrix. In separate attempts, we have carried on the Mueller matrix transformation (MMT) study, which has led to three independent structural-related parameters. Details of this study have been given in a paper submitted for publication, but the conclusion is summarized here. We analyze the backscattering Mueller matrix of a sample containing silk strands, then fit the azimuth angular-dependent elements to some unique trigonometric curves in Monte Carlo simulations. Observation of different Mueller matrix elements reveals that, an amplitude factor t , a direction factor x , and an offset factor b can be acquired:

$$\begin{aligned} t &= \frac{\sqrt{(m_{22} - m_{33})^2 + (m_{23} + m_{32})^2}}{2}, \\ \tan(4x) &= \frac{m_{23} + m_{32}}{m_{22} - m_{33}}, \\ b &= \frac{m_{22} + m_{33}}{2}, \\ A &= \frac{2b \cdot t}{b^2 + t^2} \in [0, 1]. \end{aligned}$$

Apparently, the factor t is affected by the magnitude of the anisotropy, and the direction of the alignments is reflected in factor x . The factor b is correlated to many properties of the samples, which may include the size distributions of the scatterers. What is more, the close relations between the amplitude factor t and offset parameter b provide us a normalized factor A , which can be used as an anisotropy indicator. Both the RLPI and MMT techniques can be used for biomedical imaging purposes, however, the RLPI and MMT parameters have different advantages, which require comparisons and analysis in details for a better utility. In this paper, several biological tissue samples are prepared for both the RLPI and MMT imaging. The samples include the chicken heart, the healthy and cancerous liver tissues of mice, and the acne of human skin.

3. Results and Discussions

Figure 2 shows the experimental results of the RLPI and MMT parameters of a chicken heart sample with the lower part cut and removed to produce a cross-sectional area of the ventricle. The imaging size is about 1 cm by 1 cm. The intensity CCD image shown in Fig. 2(a) can be divided into three parts marked zone 1, zone 2 and zone 3. In zones 1 and 2, the muscle fibers are aligned perpendicular and parallel to the imaging X–Y plane, respectively. Moreover, the muscle fibers in zone 2 are concentrically well aligned around the center of the ventricle. The muscle fibers in zone 3 are randomly oriented to form an isotropic scattering area of the sample. As shown in Figs. 2(b) and 2(c), both the parameter G of RLPI method and the parameter A of MMT technique are good indicators for anisotropic structures. In Figs. 2(b) and 2(c), three parts with different magnitudes of anisotropy can be clearly discriminated. Meanwhile, the $\varphi_3/2$ and x -images of the chicken heart samples [Figs. 2(d) and 2(e)] reveal the directions of the muscle fibers. As shown in Fig. 2(e) the MMT factor x clearly shows the periodical changes of concentrically muscle fibers. However, compared to RLPI factor $\varphi_3/2$, x can only be determined to within $1/8$ of the full 2π range, while $\varphi_3/2$ can be used to determine all the angular distributions. Therefore, different types of Mueller matrix elements can be used in a ruler-vernier scheme: One may use RLPI parameter $\varphi_3/2$ for course estimations of the fiber

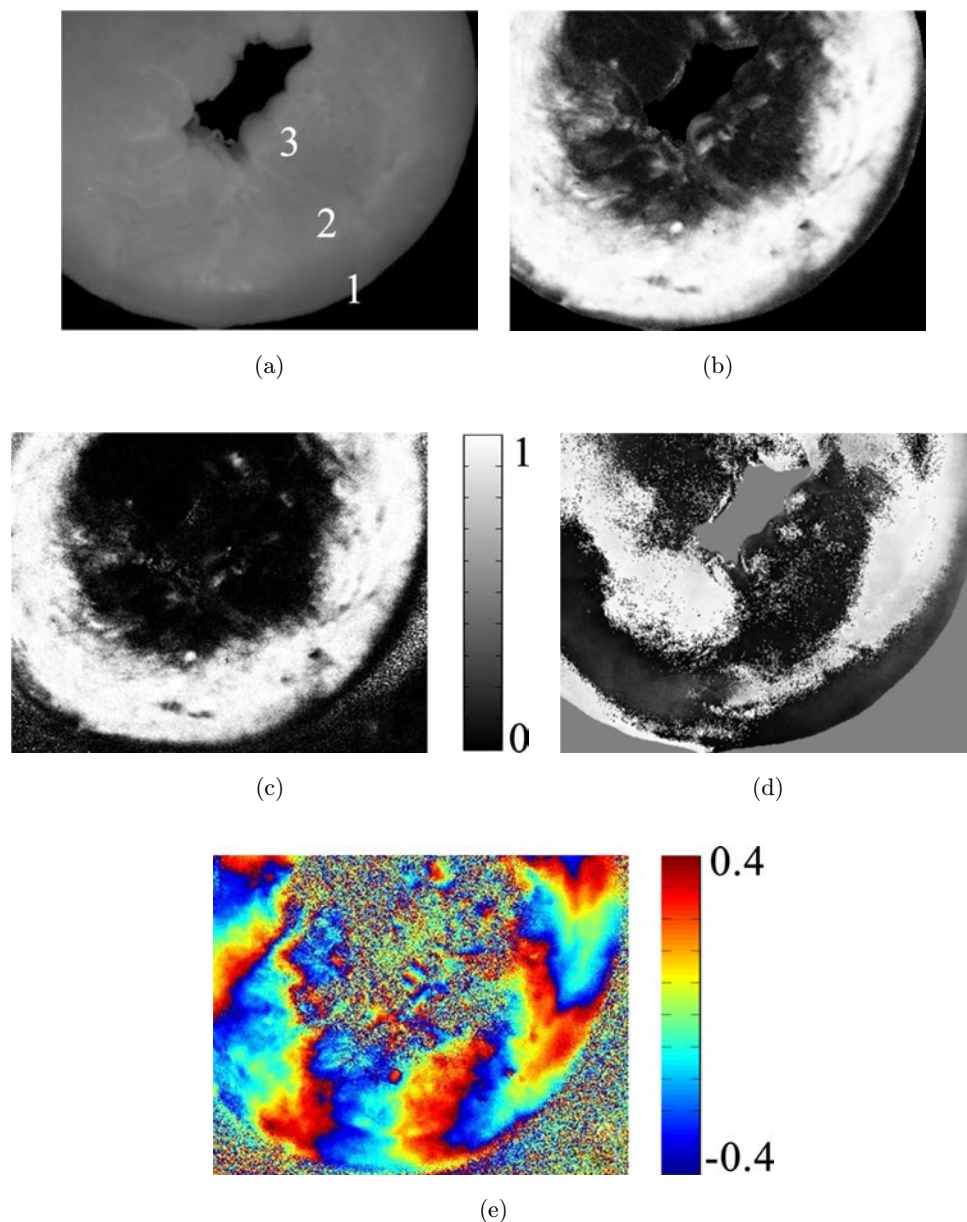


Fig. 2. Different images of the chicken heart cross-section. (a) intensity CCD image; (b) image of RLPI parameter G ; (c) image of MMT parameter A ; (d) image of RLPI parameter $\varphi_3/2$; (e) image of MMT parameter x . For the chicken heart sample, zone 1 and 2 contain the muscle fibers aligned perpendicular and parallel to the imaging X–Y plane, and the muscle fibers in zone 3 are randomly oriented.

orientation, then use x , which have smaller period and better signal-to-noise ratio, for more accurate measurements.

Both the experimental and simulated results reveal that, the RLPI parameter B and MMT factor b are sensitive to the sizes of the scatterers, especially of those smaller than the wavelength of light. However, compared to factor b , B is still correlated to the anisotropy of the tissues. For 650 nm incident light, when the diameter of the

spheres is above $1\ \mu\text{m}$, b is no longer sensitive to further changes in the size of the scatterers. A closer examination of b indicates that it can be used to differentiate different contributions by smaller and larger scatterers in a multi-dispersed isotropic scattering system. If a turbid medium contains two types of spherical scatterers, one is smaller and the other one is bigger in reference to the wavelength of the light, b only responds monotonously to the density changes of the smaller particle. In biological

tissues, there are mainly two types of scatterers: The nuclei and the organelles. The diameter of the cell nuclei is in the multi micron scale, but the intracellular organelles are often in submicron scale. In human tissues, the crowded metabolism-related organelles are the warning signs for precancerous cells.¹⁻³ The sensitive response of b to the density changes of small scatterers makes it a potential indicator for early stage cancer diagnosis. Figure 3 shows the b and A experimental results of cancerous mouse liver tissues. Anatomically, both healthy and cancerous liver tissues are isotropic but the latter contains much more mitochondrion of diameter

$0.4\text{--}0.8\ \mu\text{m}$. Therefore, compared to normal liver tissues, b is much bigger for cancerous tissue. Meanwhile, for both the liver and cancer cells, A is close to 0. The experimental results show the ability of the MMT parameters for tissue discrimination and early-stage cancer diagnosis.

Besides the *ex vivo* experiments for biological tissues, we also conducted *in vivo* MMT measurements for human tissues. Figure 4 shows the forehead skin of a male volunteer, with acne in the center. The acne area is marked by a yellow circle frame. The other parts in the figure are normal skin areas. As shown in Fig. 4(b), the edge of

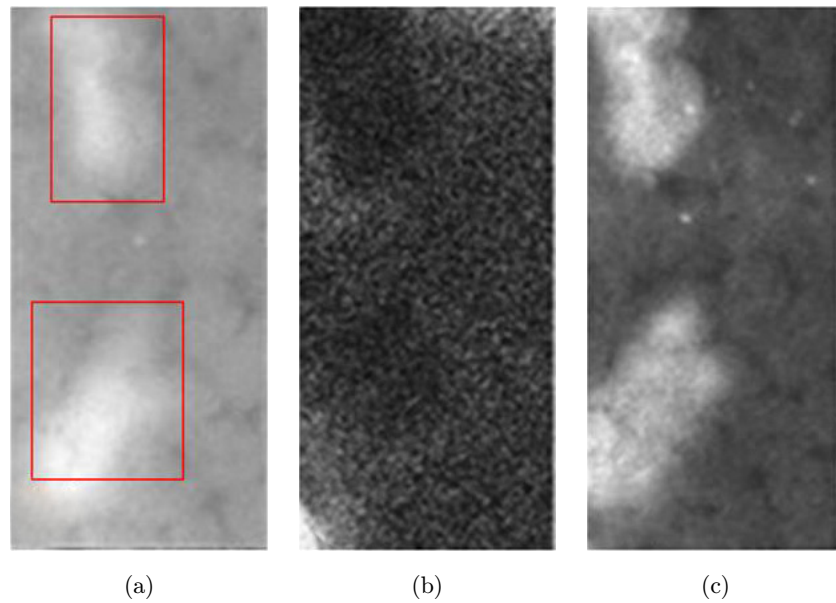


Fig. 3. Different images of the healthy and cancerous liver tissues of a mouse. (a) Intensity CCD image; (b) image of MMT parameter A ; (c) image of MMT parameter b . The cancerous tissue area is marked by red square frames.

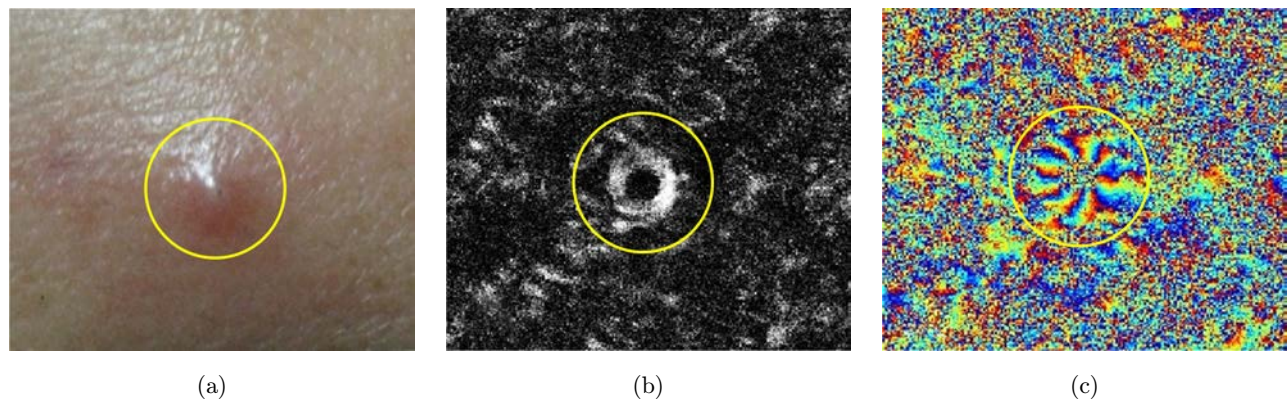


Fig. 4. Different images of the forehead skin with acne. (a) Intensity image; (b) image of MMT parameter A ; (c) image of MMT parameter x . The acne area is marked by a yellow circle frame.

pathological area has a higher value of A , which may be caused by increased collagen fibers at the early stage of wound healing. And a periodic color pattern [Fig. 4(c)] similar with the Fig. 2(e) implies these regenerate fibers are radially arranged. This simple lesion imaging show the capability of the MMT parameters to identify the location or the edge areas of the pathological tissues and even to evaluate the disease processes. All the tissue experiments results above have testified the potential utility of the MMT and RLPI parameters for biomedical imaging. However, it should be noted that the present Mueller matrix transformation is incomplete. There are signs that the factors can be further decomposed. If more complicated models are adopted in the simulation to take into account of more structural or optical properties of the media, such as linear or circular birefringence and dichroism, we may carry on the above transformation procedure further to obtain more parameters which link up the Mueller matrix elements to the properties of the media.

4. Conclusion

In summary, by conducting both the rotating linear polarization imaging (RLPI) and Mueller matrix transformation (MMT) measurements of different biological tissue samples, we have compared the extracted parameters, and testified the capability of the Mueller matrix polarimetry for the anisotropic scattering media. What is more, three parameters extracted from MMT technique are analyzed, tissue experiments show that the factors A , x and b are closely related to the structural characteristics of the turbid scattering media, including the anisotropy degree, the sizes of the scatterers, and the angular distributions of the fibers. Meanwhile, we have found that the existing parameters may be refined into some other more detailed structural parameters. For instance, in tissues both the fibrous scatterers and linear birefringence can lead to the changes of the anisotropy. A preliminary analysis reveals a possibility for a separation of the effects coming from scattering and birefringence. In short, the present results and conclusions in this paper may provide a potential method for pre-cancerous and early stage cancerous tissues detection. Yet there are more necessary studies needed for a correlation between our work and pathology knowing.

Acknowledgments

This work was supported by the National Natural Science Foundation of China (NSFC) Grants No. 10974114, 11174178, 41106034.

References

1. L. Qiu, D. K. Pleskow, R. Chuttani, E. Vitkin, J. Leyden, N. Ozden, S. Itani, L. Guo, A. Sacks, J. D. Goldsmith, M. D. Modell, E. B. Hanlon, I. Itzkan, L. T. Perelman, "Multispectral scanning during endoscopy guides biopsy of dysplasia in Barrett's esophagus," *Nat. Med.* **16**, 603–607 (2010).
2. R. S. Gurjar, V. Backman, L. T. Perelman, I. Georgakoudi, K. Badizadegan, I. Itzkan, R. R. Dasari, M. S. Feld, "Imaging human epithelial properties with polarized lightscattering spectroscopy," *Nat. Med.* **7**, 1245–1248 (2001).
3. M. Antonelli, A. Pierangelo, T. Novikova, P. Validire, A. Benali, B. Gayet, A. D. Martino, "Mueller matrix imaging of human colon tissue for cancer diagnostics: How Monte Carlo modeling can help in the interpretation of experimental data," *Opt. Express* **18**, 10200–10208 (2010).
4. B. D. Cameron, M. J. Rakovic, M. Mehrubeoglu, G. W. Kattawar, S. Rastegar, L. V. Wang, G. L. Cote, "Measurement and calculation of the two-dimensional backscattering Mueller matrix of a turbid medium," *Opt. Lett.* **23**, 485–487 (1998).
5. J. Dillet, C. Baravian, F. Caton, A. Parker, "Size determination by use of two-dimensional Mueller matrices backscattered by optically thick random media," *Appl. Opt.* **45**, 4669–4678 (2006).
6. B. D. Cameron, Y. Li, A. Nezhuvinal, "Determination of optical scattering properties in turbid media using Mueller matrix imaging," *J. Biomed. Opt.* **11**, 054031 (2006).
7. T. L. Yun, N. Zeng, W. Li, D. Z. Li, X. Y. Jiang, H. Ma, "Monte Carlo simulation of polarized photon scattering in anisotropic media," *Opt. Express* **17**, 16590–16602 (2009).
8. H. H. He, N. Zeng, R. Liao, T. L. Yun, W. Li, Y. H. He, H. Ma, "Application of sphere-cylinder scattering model to skeletal muscle," *Opt. Express* **18**, 15104–15112 (2010).
9. H. H. He, N. Zeng, W. Li, T. L. Yun, R. Liao, Y. H. He, H. Ma, "Two-dimensional backscattering Mueller matrix of sphere-cylinder scattering medium," *Opt. Lett.* **35**, 2323–2325 (2010).
10. S. Lu, R. Chipman, "Interpretation of Mueller matrices based on polar decomposition," *J. Opt. Soc. Am. A* **13**, 1106–1113 (1996).

11. N. Ghosh, M. F. G. Wood, I. A. Vitkin, "Influence of the order of the constituent basis matrices on the Mueller matrix decomposition-derived polarization parameters in complex turbid media such as biological tissues," *Opt. Commun.* **283**, 1200–1208 (2010).
12. M. Dubreuil, P. Babilotte, L. Martin, D. Sevrain, S. Rivet, Y. L. Grand, G. L. Brun, B. Turlin, B. L. Jeune, "Mueller matrix polarimetry for improved liver fibrosis diagnosis," *Opt. Lett.* **37**, 1061–1063 (2012).
13. N. Zeng, X. Y. Jiang, Q. Gao, Y. H. He, H. Ma, "Linear polarization difference imaging and its potential applications," *Appl. Opt.* **48**, 6734–6739 (2009).
14. R. Liao, N. Zeng, X. Y. Jiang, D. Z. Li, T. L. Yun, Y. H. He, H. Ma, "Rotating linear polarization imaging technique for anisotropic tissues," *J. Biomed. Opt.* **15**, 036014–036014-6 (2010).
15. C. F. Bohren, D. R. Huffman, *Absorption and Scattering of Light by Small Particles* (Wiley, New York, 1983).